

Spa3R: Predictive Spatial Field Modeling for 3D Visual Reasoning

Haoyi Jiang^{1*} Liu Liu^{2†} Xinjie Wang² Yonghao He³
Wei Sui³ Zhizhong Su² Wenyu Liu¹ Xinggang Wang^{1‡}

¹Huazhong University of Science & Technology ²Horizon Robotics ³D-Robotics

Abstract

*While Vision-Language Models (VLMs) exhibit exceptional 2D visual understanding, their ability to comprehend and reason about 3D space—a cornerstone of spatial intelligence—remains superficial. Current methodologies attempt to bridge this domain gap either by relying on explicit 3D modalities or by augmenting VLMs with partial, view-conditioned geometric priors. However, such approaches hinder scalability and ultimately burden the language model with the ill-posed task of implicitly reconstructing holistic 3D geometry from sparse cues. In this paper, we argue that spatial intelligence can emerge inherently from 2D vision alone, rather than being imposed via explicit spatial instruction tuning. To this end, we introduce **Spa3R**, a self-supervised framework that learns a unified, view-invariant spatial representation directly from unposed multi-view images. Spa3R is built upon the proposed Predictive Spatial Field Modeling (PSFM) paradigm, where Spa3R learns to synthesize feature fields for arbitrary unseen views conditioned on a compact latent representation, thereby internalizing a holistic and coherent understanding of the underlying 3D scene. We further integrate the pre-trained Spa3R Encoder into existing VLMs via a lightweight adapter to form **Spa3-VLM**, effectively grounding language reasoning in a global spatial context. Experiments on the challenging VSI-Bench demonstrate that Spa3-VLM achieves state-of-the-art accuracy of 58.6% on 3D VQA, significantly outperforming prior methods. These results highlight PSFM as a scalable path toward advancing spatial intelligence. Code is available at <https://github.com/hustvl/Spa3R>.*

1. Introduction

The ability to perceive and reason about the 3D world is fundamental to spatial intelligence, underpinning applica-

tions from autonomous navigation to robotic manipulation. Despite the remarkable progress of Vision-Language Models (VLMs) in interpreting 2D image content, their comprehension of 3D geometry and spatial relations remains superficial [39]. This limitation stems from the 2D nature of their pre-training, which lacks the necessary inductive biases to construct a coherent spatial manifold across multiple views.

To endow VLMs with 3D spatial awareness, a straightforward strategy involves scaling training with massive multi-view data paired with spatial Question-Answer (QA) annotations. However, this approach imposes immense data demands, as it essentially requires the language model to acquire spatial understanding from first principles. An alternative line of work [5, 10] incorporates explicit 3D modalities such as LiDAR point clouds. While being geometrically grounded, their reliance on specialized sensors severely restricts real-world scalability and applicability.

Recent advances in geometry foundation models [34, 35] have inspired methods that augment VLMs with geometric priors extracted from multiple views [9, 38, 46]. However, these methods typically provide the VLM with only partial, view-conditioned features from a limited set of views due to computational constraints, leaving significant spatial context unobserved. Consequently, the VLMs are tasked with the fundamentally ill-posed problem of implicitly reconstructing a holistic 3D scene from partial visual tokens, under the sparse supervision provided by instruction tuning.

In contrast, we propose that spatial intelligence can emerge inherently from 2D vision alone through predictive modeling, dispensing with explicit spatial instruction tuning—akin to how humans develop spatial awareness from multi-view and motion observation. To this end, we introduce Spa3R, a novel self-supervised framework built upon our Predictive Spatial Field Modeling (PSFM) paradigm. The Spa3R Encoder embeds a 3D scene from unposed context views into a unified, view-invariant spatial representation. A corresponding decoder then synthesizes the spatial feature field for arbitrary, unseen views conditioned on this latent representation. This predictive information bottleneck compels the encoder to capture the intrinsic 3D geometry, spatial layout, and semantic relationships of the scene,

*Intern at D-Robotics: haoyi_jiang@hust.edu.cn

†Project leader

‡Corresponding author: xgwang@hust.edu.cn

yielding a holistic understanding that extends beyond the observed images.

By decoupling spatial representation learning from reasoning, the pre-trained Spa3R encoder serves as a versatile plug-in module. We integrate it into Qwen2.5-VL [1] via a lightweight Residual Cross-Attention Adapter to form Spa3-VLM, enabling the VLM’s native visual features to actively query the unified spatial context. This design preserves the generalization capabilities of the base VLM while efficiently grounding its reasoning in 3D space. Extensive experiments demonstrate that Spa3-VLM achieves state-of-the-art performance across multiple spatial reasoning benchmarks, notably achieving 58.6% accuracy on the challenging VSI-Bench [39]. These results establish PSFM as a novel and scalable paradigm for advancing spatial intelligence.

Our contributions are threefold:

- We identify a fundamental bottleneck in existing VLMs for spatial reasoning: relying on the language model to implicitly reconstruct 3D scenes from partial, view-conditioned features constitutes an inefficient and ill-posed learning objective.
- We propose **Spa3R**, a self-supervised framework based on Predictive Spatial Field Modeling (PSFM) that learns a unified, view-invariant spatial representation by synthesizing feature fields for arbitrary novel views, thereby internalizing intrinsic geometry and spatial layout of the scene.
- We present **Spa3-VLM**, which integrates the pre-trained Spa3R Encoder to ground VLM reasoning in a holistic spatial context. Extensive experiments on VSI-Bench showcase significant performance improvement, highlighting PSFM as a scalable and effective path toward general spatial intelligence.

2. Related Work

2.1. 3D Reconstruction and Scene Representation

Recent advances in 3D reconstruction have undergone a fundamental shift from scene-specific optimization toward generalizable, feed-forward inference. Neural Radiance Fields (NeRF) [24] revolutionized scene representation with implicit neural fields, yet require costly per-scene training. Subsequent works, such as pixelNeRF [43] and MVS-NeRF [4], introduced conditional neural fields to learn generalizable 3D priors across multiple scenes. This feed-forward paradigm has recently extended to 3D Gaussian Splatting [3] and occupancy prediction [13, 15, 26], facilitating efficient 3D perception from multi-view images.

In parallel, the rise of large-scale pre-training has fostered the development of geometry foundation models. The DUST3R [18, 35] and VGGT [34, 36] series demonstrated robust 3D reconstruction by effectively unifying the estima-

tion of diverse 3D attributes including point maps, depth, and camera parameters from unposed images. These foundation models provide powerful, spatially grounded priors, inspiring hybrid frameworks [8, 30, 41] that combine such geometric estimation with rendering-based refinement for 3D reconstruction and semantic understanding.

A recent, transformative trend involves pure Transformer architectures for Novel View Synthesis (NVS), spearheaded by LVSM [17] and its variants [16, 33]. Eschewing explicit 3D inductive biases, these models leverage the representational capacity and scaling properties of Transformers to implicitly infer geometric structure from 2D data. Spa3R draws inspiration from this predictive paradigm but diverges fundamentally in objective. While LVSM prioritizes pixel-level synthesis for high-fidelity visual reconstruction, our PSFM framework targets representation learning by predicting spatially-grounded feature fields. It thus encapsulates the scene’s intrinsic geometry and semantic relationships within a unified, view-invariant latent space optimized for downstream spatial reasoning tasks.

2.2. Vision-Language Models for 3D Reasoning

While VLMs excel at 2D image-text alignment, extending them to the spatial domain remains challenging. Early approaches relied on explicit 3D modalities, either through object-centric representations [11, 37] or by directly processing point clouds [5, 10, 12] to ground language in 3D space. While these approaches benefit from strong geometric grounding, their dependence on specialized sensors (*e.g.*, LiDAR) or pre-processed 3D data severely restricts their real-world scalability and applicability.

Recent research has shifted toward inferring 3D understanding from widespread 2D video or multi-view data. GPT4Scene [28] reconstructs Bird’s-Eye View (BEV) representations from video features to capture spatio-temporal context, while approaches such as VG-LLM [46], Spatial-MLLM [38], and VLM3R [9] augment VLMs with view-conditioned priors extracted from geometry foundation models.

Nevertheless, a fundamental bottleneck persists: these approaches typically expose the VLM to only partial, view-conditioned geometric cues, offloading the burden of holistic 3D reconstruction to the language model under sparse supervision. In contrast, our work addresses this limitation by introducing Predictive Spatial Field Modeling (PSFM), a self-supervised paradigm that explicitly learns a unified, view-invariant spatial representation, providing a robust and coherent foundation that empowers complex spatial reasoning.

3. Method

In this section, we first outline the theoretical formulation of Predictive Spatial Field Modeling (PSFM) in Sec. 3.1.

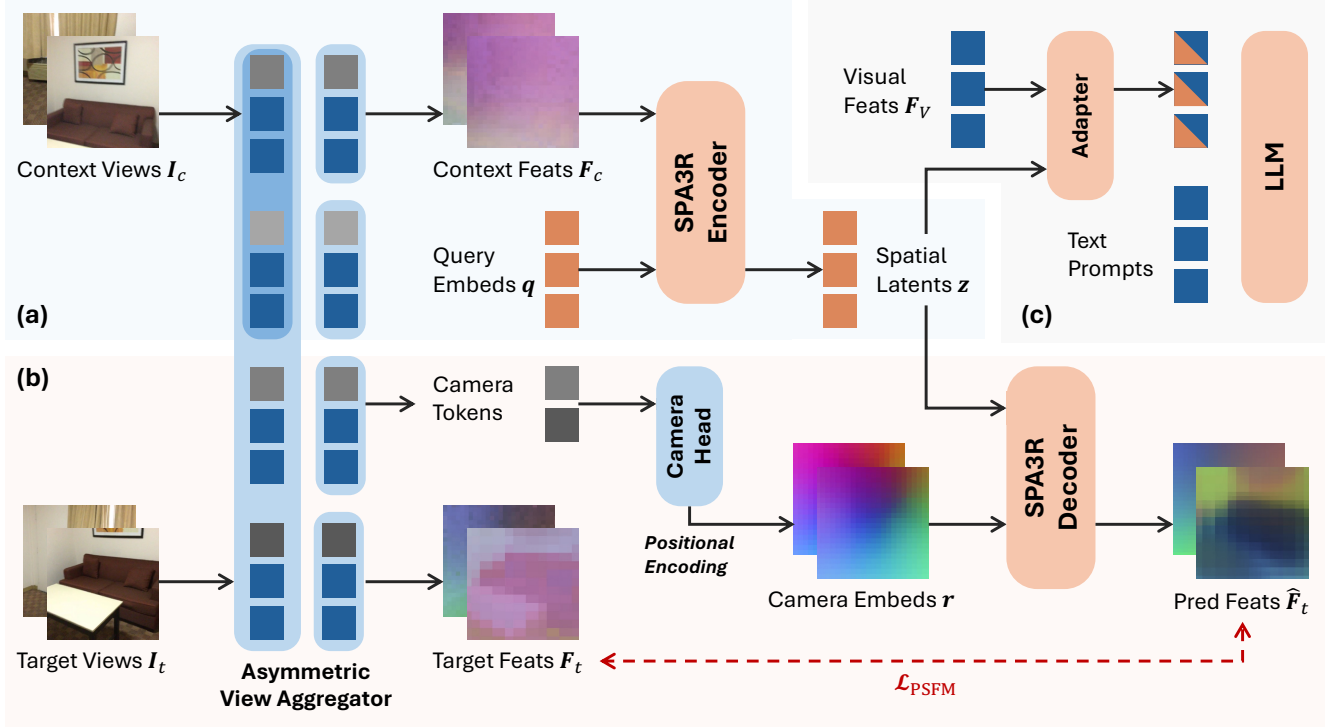


Figure 1. **Overview of the Spa3R framework and Spa3-VLM integration.** (a) The Spa3R Encoder maps unposed context views to a unified, view-invariant spatial latent representation z . (b) The Spa3R Decoder synthesizes target features \hat{F}_t for arbitrary unseen views, conditioned on the spatial latent z and target camera embeddings r . (c) For downstream spatial reasoning, the pre-trained Spa3R Encoder is integrated into a VLM to generate spatial representation z . A lightweight Adapter fuses the VLM’s native visual features F_V with spatial latent z via cross-attention, effectively grounding its reasoning in spatial context.

We then elaborate on the Spa3R architecture in Sec. 3.2. Subsequently, we describe the integration of the pre-trained Spa3R representation into Vision-Language Models to form Spa3-VLM in Sec. 3.3. An overview of the framework is illustrated in Fig. 1.

3.1. Predictive Spatial Field Modeling

We formulate 3D spatial understanding as a Spatial Field Modeling problem. We conceptualize a 3D scene as a continuous spatial feature field f , a function mapping any view-point defined by camera pose $v \in \mathcal{V}$ to its corresponding view-centric feature map $F \in \mathcal{F}$:

$$f : \mathcal{V} \rightarrow \mathcal{F}. \quad (1)$$

The goal of PSFM is to infer the low-dimensional spatial manifold—which encapsulates the scene’s intrinsic geometric structure—from a sparse set of N_C context views $C = \{(v_c, F_c)\}_{c=1}^{N_C}$. We formally frame this problem as a Neural Process. Specifically, we leverage an amortized encoder E_ϕ to encode the context set C into a unified latent variable z . This variable z serves as a holistic representation of the spatial manifold, parameterizing the intrinsic

properties of the scene. A decoder D_θ then acts as a conditional neural field that reconstructs the target view features \hat{F}_t for arbitrary target poses v_t conditioned on z :

$$z = E_\phi(C) = E_\phi\left(\{(v_c, F_c)\}_{c=1}^{N_C}\right), \quad (2)$$

$$\hat{F}_t = D_\theta(v_t|z). \quad (3)$$

During the training phase, we sample a set of views S from each scene and randomly partition it into a context set C and a target set T . The learning objective is to minimize the distance between the predicted features \hat{F}_t and their ground-truth counterparts F_t :

$$\mathcal{L}_{\text{PSFM}} = \mathbb{E}_{C, T \sim S} \left[\sum_{t \in T} \text{dist}(D_\theta(v_t|E_\phi(C)), F_t) \right]. \quad (4)$$

Theoretically, PSFM establishes an information bottleneck that disentangles intrinsic spatial representation from extrinsic, view-conditioned properties. By forcing the encoder E_ϕ to support the synthesis of features at arbitrary points on the manifold via a single latent z , the model is compelled to internalize the complete 3D geometry and spatial layout of the scene.

3.2. Learning a Unified Spatial Representation

Spa3R instantiates the PSFM paradigm using a specialized encoder-decoder architecture composed of an Asymmetric View Aggregator, a Spa3R Encoder, and a Spa3R Decoder.

Asymmetric View Aggregator A critical prerequisite for PSFM is the construction of a canonical spatial feature field f where context features F_c and target features F_t are spatially aligned. To achieve this, we introduce an Asymmetric View Aggregator, which effectively adapts the pre-trained VGGT [34] to extract spatially-aligned features using its powerful global attention mechanism. We employ an asymmetric attention masking strategy in the global attention layers of VGGT to strictly prevent information leakage from target views to context views. Given a batch of context views C and target views T , we construct a view mask $M \in \{0, -\infty\}^{L \times L}$ applied to the attention logits, where L denotes the total sequence length. Specifically, target views are allowed to attend to all views ($C \cup T$), whereas context views are restricted to attending only to other context views. Formally, for a query patch from view i and a key patch from view j :

$$M_{ij} = \begin{cases} 0 & \text{if } i \in T \text{ or } j \in C, \\ -\infty & \text{otherwise.} \end{cases} \quad (5)$$

This mechanism ensures that context features F_c are computed independently of the targets, while target features F_t and their corresponding camera poses v_t are spatially grounded in the same coordinate system.

Spa3R Encoder The Spa3R Encoder E_ϕ is a Transformer designed to encapsulate the context features F_c into a compact representation $z \in \mathbb{R}^{N_q \times D}$. We initialize N_q learnable query embeddings q . These queries are concatenated with the context features F_c into a single sequence and processed through Transformer layers to iteratively refine the queries by aggregating information from the context, yielding the final spatial representation z :

$$H = \text{Transformer}(\text{Concat}[q, F_c]), \quad (6)$$

$$z = H[: N_q]. \quad (7)$$

Spa3R Decoder The Spa3R Decoder D_θ synthesizes the target features \hat{F}_t conditioned on the spatial latent z and the target camera pose v_t . This process involves two key geometric mechanisms: ray-based querying and relative 3D positional encoding. First, to encode the embeddings of the target view frustum, we generate camera-space ray directions d for each homogeneous pixel coordinate \tilde{u} using the estimated intrinsics K :

$$d = \text{Normalize}(K^{-1}\tilde{u}), \quad (8)$$

These ray directions d are mapped to initial camera embeddings r via a linear projection.

Second, to explicitly model the geometric relationship between the target view and the spatial context, we employ PRoPE [22] within the decoder. PRoPE encodes the relative transformation between cameras directly into the attention mechanism. The attention calculation between query Q , key K , and value V is computed as:

$$O_i = \sum_j \text{softmax}\left(\frac{Q_i^\top \mathcal{T}_{ij} K_j}{\sqrt{d}}\right) \mathcal{T}_{ij} V_j, \quad (9)$$

$$\mathcal{T}_{ij} = D_i^{\text{PRoPE}} (D_j^{\text{PRoPE}})^{-1}, \quad (10)$$

where D^{PRoPE} is the relative positional encoding matrix encapsulating the 3D projection matrices and intra-view 2D RoPE. The target view camera embeddings r then query the spatial context z through the Transformer Decoder D_θ to synthesize the target features \hat{F}_t :

$$H' = \text{Transformer}(\text{Concat}[r, z]), \quad (11)$$

$$\hat{F}_t = H'[: -N_q]. \quad (12)$$

Losses The Spa3R framework is trained end-to-end to minimize the reconstruction error of the target features. Specifically, the target features are composed of geometric features from the Asymmetric View Aggregator and semantic features from a frozen DINOv3 [29] backbone (omitted from the figure for brevity). The incorporation of semantic features serves as an auxiliary objective, explicitly encouraging the encoder to capture high-level semantic abstractions alongside geometric structures. To this end, the decoder employs separate geometric and semantic prediction heads. We apply a consistent loss formulation independently to both heads, combining the L1 distance and Cosine Similarity:

$$\mathcal{L}(\hat{F}_t, F_t) = \|\hat{F}_t - F_t\|_1 + \left(1 - \frac{\hat{F}_t \cdot F_t}{\|\hat{F}_t\|_2 \cdot \|F_t\|_2}\right). \quad (13)$$

The total training objective is the sum of the reconstruction losses from both the geometric and semantic heads.

3.3. Grounding Reasoning in Spatial Context

To endow Vision-Language Models with spatial intelligence, we integrate the pre-trained, frozen Spa3R Encoder into Qwen2.5-VL [1] to create Spa3-VLM. As depicted in Fig. 1(c), we utilize a lightweight Residual Cross-Attention Adapter to fuse the unified, view-invariant Spa3R latent representation z with the VLM’s native 2D visual features F_V for efficient cross-modal alignment. Native visual features F_V are enriched by querying the 3D spatial context z , followed by a zero-initialized MLP projector and a residual

Model	Avg.	Obj. Count	Abs. Dist.	Obj. Size	Room Size	Rel. Dist.	Rel. Dir.	Route Plan	Appr. Order
		Numerical Answer				Multiple-Choice Answer			
<i>Proprietary Models</i>									
GPT-4o [14]	34.0	46.2	5.3	43.8	38.2	37.0	41.3	31.5	28.5
Gemini-1.5-Flash [31]	42.1	49.8	30.8	53.5	54.4	37.7	41.0	31.5	37.8
Gemini-1.5-Pro [31]	45.4	56.2	30.9	64.1	43.6	51.3	46.3	36.0	34.6
<i>Open-source Models</i>									
InternVL2-8B [6]	37.5	31.3	29.0	48.9	44.2	38.0	33.4	28.9	46.4
VILA-1.5-8B [23]	28.9	17.4	21.8	50.3	18.8	32.1	34.8	31.0	24.8
LLaVA-Video-7B [45]	35.6	48.5	14.0	47.8	24.2	43.5	42.4	34.0	30.6
LLaVA-OneVision-7B [19]	32.4	47.7	20.2	47.4	12.3	42.5	35.2	29.4	24.4
Qwen2.5VL-3B [1]	30.6	24.3	24.7	31.7	22.6	38.3	41.6	26.3	21.2
Qwen2.5VL-7B [1]	33.0	40.9	14.8	43.4	10.7	38.6	38.5	33.0	29.8
<i>Spatial Models</i>									
Spatial-MLLM-4B [38]	48.4	65.3	34.8	63.1	45.1	41.3	46.2	33.5	46.3
VG-LLM-4B [46]	47.3	66.0	37.8	55.2	59.2	44.6	45.6	33.5	36.4
VG-LLM-8B [46]	50.7	67.9	37.7	58.6	<u>62.0</u>	46.6	40.7	32.4	59.2
Cambrian-S-3B [40]	<u>57.3</u>	70.7	40.6	<u>68.0</u>	46.3	64.8	61.9	27.3	78.8
Spa3-VLM-4B (Ours)	58.6	<u>69.0</u>	<u>39.3</u>	70.6	62.8	<u>57.9</u>	<u>59.5</u>	36.1	<u>73.6</u>

Table 1. Quantitative comparison on the VSI-Bench [39] spatial reasoning benchmark.

connection to preserve the VLM’s pre-trained knowledge:

$$\mathbf{F}_{\text{fused}} = \text{CrossAttn}(q = \mathbf{F}_V, k = \mathbf{z}, v = \mathbf{z}), \quad (14)$$

$$\mathbf{F}'_V = \mathbf{F}_V + \text{MLP}(\mathbf{F}_{\text{fused}}). \quad (15)$$

The spatially enriched features \mathbf{F}'_V are then concatenated with text embeddings and fed into the language model. The adapter and the language model are fine-tuned with spatial instruction tuning, while the Spa3R encoder and the VLM’s vision encoder remain frozen, retaining the generalization capabilities of the base VLM while efficiently grounding its reasoning in the 3D spatial context.

4. Experiments

In this section, we conduct extensive experiments to evaluate the effectiveness of our proposed approach. We first detail the experimental setup, including datasets and evaluation benchmarks, in Sec. 4.1. We then provide implementation details for both Spa3R pre-training and Spa3-VLM instruction tuning in Sec. 4.2. Subsequently, we report quantitative results on VSI-Bench and other spatial reasoning benchmarks in Sec. 4.3, followed by ablation studies and qualitative analyses in Sec. 4.4 and Sec. 4.5.

4.1. Setup

Pre-training Datasets We pre-train the Spa3R framework on a combination of ScanNet [7] and ScanNet++ [42]. These large-scale indoor scene datasets provide rich RGB-

D video sequences captured from diverse real-world environments, with each dataset containing over 1,000 uniquely scanned scenes.

Evaluation Benchmarks Our primary evaluation is conducted on VSI-Bench [39], a challenging benchmark designed to assess the visual-spatial intelligence of VLMs from video inputs. It comprises over 5,000 question-answer pairs derived from 288 real-world indoor scene videos, categorized into three tasks: configurational, measurement estimation, and spatiotemporal. Evaluation is performed using the Accuracy metric for Multiple-Choice Answer (MCA) tasks, and Mean Relative Accuracy (MRA) for Numerical Answer (NA) tasks measuring numerical precision by averaging relative accuracy across a spectrum of confidence thresholds. To comprehensively assess the cross-domain generalization capabilities of our model, we further extend our evaluation to several 3D spatial reasoning benchmarks with single or multiple image inputs including CV-Bench [32], SPAR-Bench [44], and ViewSpatial-Bench [20].

Instruction-Tuning Datasets For the video-centric VSI-Bench, we fine-tune Spa3-VLM on the VSI-590K [40] dataset. For image-based benchmarks, we construct a composite training set comprising SPAR-234K [44], LLaVA-Hound [45], and the VLM3R training data [9] aligned with prior literature.

Model	CV			SPAR	ViewSpa.
	2D	3D	Avg.		
Qwen2.5-VL-3B	69.1	72.2	70.6	24.6	35.6
SpatialLadder-3B [21]	<u>72.4</u>	74.9	73.7	34.4	44.2
Spatial-MLLM-4B	-	-	<u>73.8</u>	35.1	43.6
SpatialThinker-3B [2]	71.0	<u>76.3</u>	73.6	-	-
SpaceR-7B [25]	-	-	-	<u>37.6</u>	37.3
Spa3-VLM (Ours)	72.9	78.3	75.6	58.4	43.9

Table 2. Quantitative comparison across diverse benchmarks.

4.2. Implementation Details

Spa3R Pre-training We initialize the Asymmetric View Aggregator and the camera head with pre-trained weights from VGGT [34], which remain frozen during training. The reconstruction target comprises both geometric features from the Asymmetric View Aggregator and semantic features from DINOv3 [29] to facilitate holistic scene understanding. The Spa3R Encoder and Decoder are implemented as 6-layer Transformers with a hidden dimension of $D = 768$. We employ $N_q = 256$ learnable query embeddings to form the spatial latent representation.

The Spa3R model is pre-trained for 80K steps using the AdamW optimizer with a learning rate of 1×10^{-3} . In each iteration, we sample 4 to 12 views from a scene, randomly designating half of the views as context views masked via the asymmetric attention, and the remainder as target views. Training is conducted on 8 NVIDIA 5090 GPUs.

Spa3-VLM Instruction Tuning We adopt Qwen2.5-VL-3B [1] as the base VLM. During instruction tuning, the pre-trained Spa3R Encoder and the VLM’s native vision encoder are kept frozen to preserve their learned representations. We fine-tune only the lightweight Residual Cross-Attention Adapter and the language model parameters for one epoch on the corresponding instruction-tuning datasets. This strategy prevents catastrophic forgetting of the VLM’s general capabilities while efficiently injecting the newly acquired spatial inductive biases.

4.3. Main Results

Quantitative results for VSI-Bench and additional spatial reasoning benchmarks are summarized in Tab. 1 and Tab. 2, comparing against general-purpose VLMs and recent spatially-grounded baselines. Spa3-VLM achieves a state-of-the-art average accuracy of 58.6% on VSI-Bench, surpassing existing methods across multiple benchmarks. This advantage validates our hypothesis that the holistic, view-invariant representation learned via PSFM provides a more robust foundation for 3D spatial grounding than partial, explicit geometric cues, highlighting the scalability and effectiveness of our predictive modeling paradigm.

4.4. Ablation Studies

We conduct comprehensive ablation studies on VSI-Bench to validate the core design choices of our framework.

Effectiveness of Unified Spatial Representation. To verify the necessity and superiority of our PSFM paradigm, we compare Spa3R against a baseline that directly feeds view-conditioned geometric priors (extracted from VGGT) into the VLM, akin to contemporary methods like VG-LLM [46]. As shown in Tab. 3, directly utilizing partial, view-conditioned features yields inferior reasoning performance. In contrast, our Spa3R—which explicitly models a unified, view-invariant spatial field—achieves a significant gain of +3.5%. This substantial improvement confirms that the predictive bottleneck forces the model to learn a global 3D understanding that is crucial for complex reasoning.

Spa. Repr.	Numerical	Multi-Choice	Avg.
None	58.4	43.5	50.9
VGGT	60.5	49.5	55.1
Spa3R	60.4	56.8	58.6

Table 3. Ablation on spatial representation paradigms.

Synergy of Geometric and Semantic Reconstruction Targets. We analyze the impact of different supervision signals for the Spa3R pre-training targets. Tab. 4 compares models trained with geometric features, semantic features and linguistic features, and their combination. Results indicate that using either modality in isolation yields suboptimal performance. The best performance is achieved when combining both, suggesting that robust spatial reasoning requires both explicit geometric structure and high-level semantic context.

VGGT	DINO	CLIP	Numerical	Multi-Choice	Avg.
✓			60.5	54.4	57.5
	✓		59.0	54.4	56.7
		✓	59.5	44.3	51.9
✓	✓		60.4	56.8	58.6

Table 4. Ablation on reconstruction targets for Spa3R pre-training.

Architecture for Spa3-VLM Integration. We further investigate strategies for integrating the spatial latent into the VLM. We compare our proposed Residual Cross-Attention Adapter against a naive strategy that directly appends spatial latents to the token sequence. As reported in Tab. 5, the adapter-based fusion outperforms appending by +7.5%,

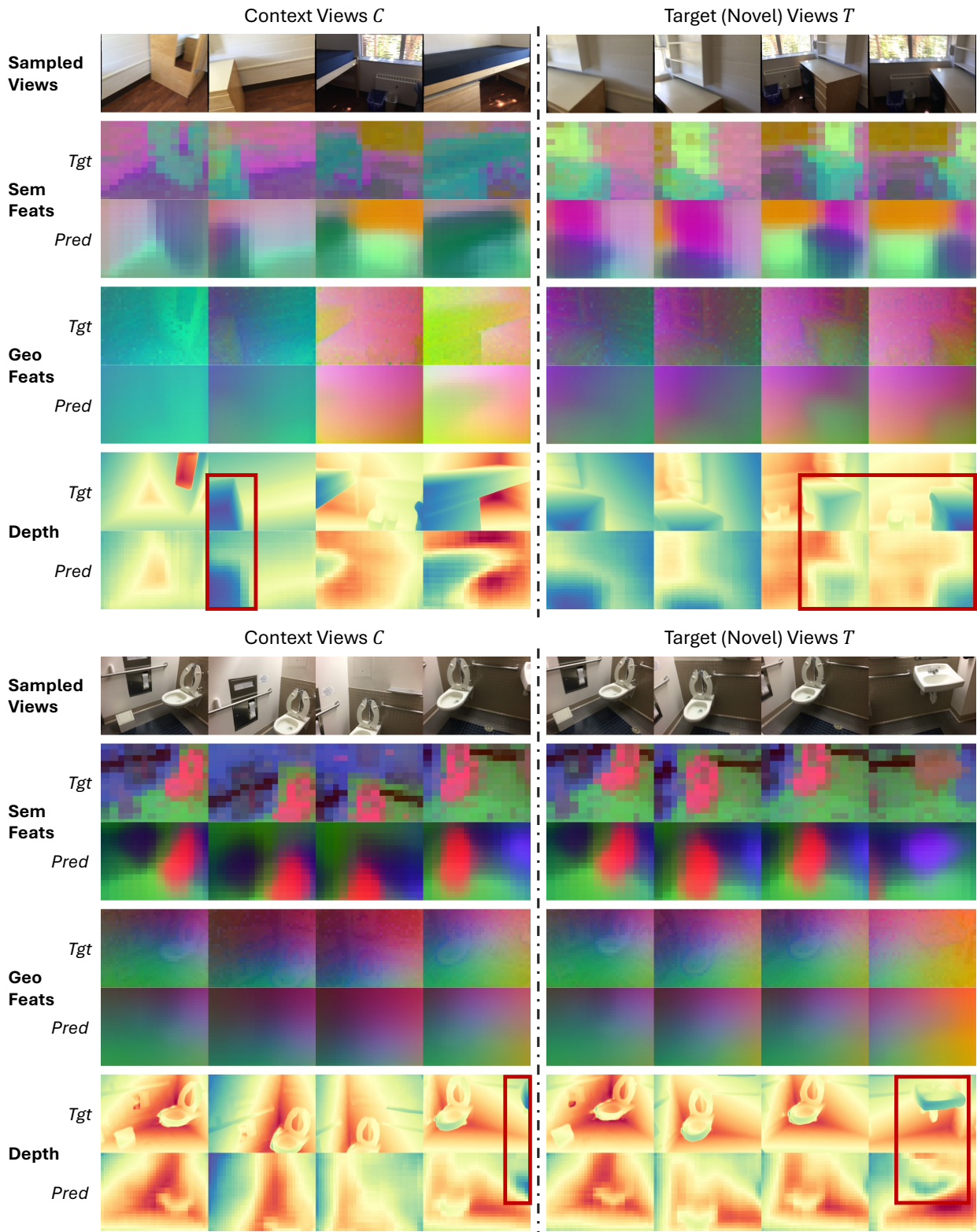


Figure 2. **Qualitative visualization of learned feature fields.** Our predictions exhibit a continuous and spatially coherent layout compared to the target features. (Colors are unaligned due to independent PCA projections necessitated by the cosine similarity supervision). Furthermore, Spa3R plausibly extrapolates features for occluded or unobserved regions (highlighted in red boxes), demonstrating that it has internalized a holistic 3D scene understanding rather than merely memorizing input views.

while appending yields only marginal gains over the baseline. We hypothesize that the pre-trained VLM tends to suffer from “modality collapse”, where the pre-trained VLM preferentially attends to its familiar native visual tokens and ignores the alien spatial latents. In contrast, the cross-attention mechanism enables the VLM to actively query relevant spatial information from the holistic representation, ensuring effective feature fusion.

Integration	Numerical	Multi-Choice	Avg.
None	58.4	43.5	50.9
Seq. Append.	58.5	43.7	51.1
Cross-Attn.	60.4	56.8	58.6

Table 5. Ablation on VLM integration architectures.

PSFM Mask Ratio. We ablate the masked ratio of target views, which fundamentally controls the difficulty of the self-supervised objective. As shown in Tab. 6, a 50% mask ratio yields peak performance. A lower mask ratio of 25% (leaving 75% context) leads to a significant performance drop of 1.1%, likely because the task becomes too trivial to enforce a holistic 3D understanding. Conversely, increasing the mask ratio to 75% (leaving only 25% context) also results in a slight performance drop, suggesting that input context may be too sparse to reliably form a coherent representation. These results indicate that a balanced split provides the optimal trade-off between contextual completeness and predictive challenge.

Mask ratio	Numerical	Multi-Choice	Avg.
25%	58.9	56.1	57.5
50%	60.4	56.8	58.6
75%	59.6	56.7	58.1

Table 6. Ablation on target view masking ratio for PSFM.

Camera Embedding Mechanism. We investigate the mechanism for conditioning the decoder on the target viewpoint. We compare the Plücker [27] coordinate embedding, an absolute pose encoding widely used in neural rendering, against the relative positional encoding provided by PRoPE [22]. As shown in Tab. 7, PRoPE outperforms Plücker coordinates by a notable margin of +1.0%. We attribute this performance gap to the inherent limitations of absolute pose encodings, which can be sensitive to variations in scene scale and coordinate origin shifts. In contrast, PRoPE injects the relative geometric transformation between context and target views directly into the attention weights, leading to more robust and geometrically consistent feature synthesis across diverse viewpoints.

Cam. Embed.	Numerical	Multi-Choice	Avg.
Plücker	59.9	55.4	57.6
PRoPE	60.4	56.8	58.6

Table 7. Ablation on camera embedding mechanisms for synthesis.

4.5. Qualitative Analysis

To provide a more intuitive understanding of the internal mechanisms and representational capacity of Spa3R, we visualize the reconstructed feature fields in Fig. 2. Specifically, we sample 8 views for each of two scenes, and compare the target geometric and semantic features against the predictions synthesized by the Spa3R Decoder.

To visualize high-dimensional feature spaces, we employ Principal Component Analysis (PCA) to project the features into RGB space. Furthermore, to explicitly observe the geometric information encoded in the representation, we perform a depth probing analysis. We attach a single, detached MLP to regress depth maps from the predicted features \hat{F}_t . Crucially, gradients from this probing head are *not* back-propagated to Spa3R, as it serves only as a diagnostic tool to reveal the intrinsic geometry present in the features.

As shown in Fig. 2, the predicted features form a continuous and coherent spatial field. The PCA visualizations exhibit consistent layouts invariant to viewpoint changes, while the depth probes recover accurate scene geometry. Notably, the model plausibly extrapolates features for occluded or unobserved regions, demonstrating that Spa3R has internalized a holistic 3D scene understanding rather than merely memorizing input views.

5. Conclusion

Vision-Language Models (VLMs) currently struggle with 3D spatial reasoning, as they are tasked with the ill-posed problem of implicitly reconstructing scenes from partial, view-conditioned features. To address this fundamental limitation, we introduce Spa3R, a self-supervised framework built upon Predictive Spatial Field Modeling (PSFM). By training the model to predictively synthesize feature fields for arbitrary novel views, Spa3R learns a unified, view-invariant spatial representation from unposed 2D images. We further bridge this capability to language reasoning by integrating the pre-trained Spa3R Encoder into a VLM through a lightweight adapter, creating Spa3-VLM to ground the language model’s reasoning in a holistic spatial context. Extensive evaluations on VSI-Bench demonstrate state-of-the-art performance, establishing PSFM as a scalable and effective paradigm for advancing spatial intelligence.

References

- [1] Shuai Bai, Keqin Chen, Xuejing Liu, Jialin Wang, Wenbin Ge, Sibao Song, Kai Dang, Peng Wang, Shijie Wang, Jun Tang, et al. Qwen2. 5-vl technical report. *arXiv preprint arXiv:2502.13923*, 2025. 2, 4, 5, 6
- [2] Hunar Batra, Haoqin Tu, Hardy Chen, Yuanze Lin, Cihang Xie, and Ronald Clark. Spatialthinker: Reinforcing 3d reasoning in multimodal llms via spatial rewards. *arXiv preprint arXiv:2511.07403*, 2025. 6
- [3] David Charatan, Sizhe Lester Li, Andrea Tagliasacchi, and Vincent Sitzmann. pixelsplat: 3d gaussian splats from image pairs for scalable generalizable 3d reconstruction. In *CVPR*, pages 19457–19467, 2024. 2
- [4] Anpei Chen, Zexiang Xu, Fuqiang Zhao, Xiaoshuai Zhang, Fanbo Xiang, Jingyi Yu, and Hao Su. Mvsnerf: Fast generalizable radiance field reconstruction from multi-view stereo. In *ICCV*, pages 14124–14133, 2021. 2
- [5] Sijin Chen, Xin Chen, Chi Zhang, Mingsheng Li, Gang Yu, Hao Fei, Hongyuan Zhu, Jiayuan Fan, and Tao Chen. Ll3da: Visual interactive instruction tuning for omni-3d understanding reasoning and planning. In *CVPR*, pages 26428–26438, 2024. 1, 2
- [6] Zhe Chen, Jiannan Wu, Wenhai Wang, Weijie Su, Guo Chen, Sen Xing, Muyan Zhong, Qinglong Zhang, Xizhou Zhu, Lewei Lu, et al. Internvl: Scaling up vision foundation models and aligning for generic visual-linguistic tasks. In *CVPR*, pages 24185–24198, 2024. 5
- [7] Angela Dai, Angel X Chang, Manolis Savva, Maciej Halber, Thomas Funkhouser, and Matthias Nießner. Scannet: Richly-annotated 3d reconstructions of indoor scenes. In *CVPR*, pages 5828–5839, 2017. 5
- [8] Zhiwen Fan, Jian Zhang, Wenyan Cong, Peihao Wang, Renjie Li, Kairun Wen, Shijie Zhou, Achuta Kadambi, Zhangyang Wang, Danfei Xu, et al. Large spatial model: End-to-end unposed images to semantic 3d. *NeurIPS*, 37: 40212–40229, 2024. 2
- [9] Zhiwen Fan, Jian Zhang, Renjie Li, Junge Zhang, Runjin Chen, Hezhen Hu, Kevin Wang, Huaizhi Qu, Dilin Wang, Zhicheng Yan, et al. Vlm-3r: Vision-language models augmented with instruction-aligned 3d reconstruction. *arXiv preprint arXiv:2505.20279*, 2025. 1, 2, 5
- [10] Yining Hong, Haoyu Zhen, Peihao Chen, Shuhong Zheng, Yilun Du, Zhenfang Chen, and Chuang Gan. 3d-llm: Injecting the 3d world into large language models. *NeurIPS*, 36: 20482–20494, 2023. 1, 2
- [11] Haifeng Huang, Yilun Chen, Zehan Wang, Rongjie Huang, Runsen Xu, Tai Wang, Luping Liu, Xize Cheng, Yang Zhao, Jiangmiao Pang, et al. Chat-scene: Bridging 3d scene and large language models with object identifiers. *NeurIPS*, 37: 113991–114017, 2024. 2
- [12] Jiangyong Huang, Silong Yong, Xiaojian Ma, Xiongkun Linghu, Puhao Li, Yan Wang, Qing Li, Song-Chun Zhu, Baoxiong Jia, and Siyuan Huang. An embodied generalist agent in 3d world. In *ICML*, 2024. 2
- [13] Yuanhui Huang, Wenzhao Zheng, Borui Zhang, Jie Zhou, and Jiwen Lu. Selfoc: Self-supervised vision-based 3d occupancy prediction. In *CVPR*, pages 19946–19956, 2024. 2
- [14] Aaron Hurst, Adam Lerer, Adam P Goucher, Adam Perelman, Aditya Ramesh, Aidan Clark, AJ Ostrow, Akila Welihinda, Alan Hayes, Alec Radford, et al. Gpt-4o system card. *arXiv preprint arXiv:2410.21276*, 2024. 5
- [15] Haoyi Jiang, Liu Liu, Tianheng Cheng, Xinjie Wang, Tianwei Lin, Zhizhong Su, Wenyu Liu, and Xinggang Wang. Gausstr: Foundation model-aligned gaussian transformer for self-supervised 3d spatial understanding. In *CVPR*, pages 11960–11970, 2025. 2
- [16] Hanwen Jiang, Hao Tan, Peng Wang, Haian Jin, Yue Zhao, Sai Bi, Kai Zhang, Fujun Luan, Kalyan Sunkavalli, Qixing Huang, et al. Rayzer: A self-supervised large view synthesis model. *arXiv preprint arXiv:2505.00702*, 2025. 2
- [17] Haian Jin, Hanwen Jiang, Hao Tan, Kai Zhang, Sai Bi, Tianyuan Zhang, Fujun Luan, Noah Snavely, and Zexiang Xu. LVSM: A large view synthesis model with minimal 3d inductive bias. In *ICLR*, 2025. 2
- [18] Vincent Leroy, Yohann Cabon, and Jérôme Revaud. Grounding image matching in 3d with mast3r. In *ECCV*, pages 71–91, 2024. 2
- [19] Bo Li, Yuanhan Zhang, Dong Guo, Renrui Zhang, Feng Li, Hao Zhang, Kaichen Zhang, Peiyuan Zhang, Yanwei Li, Ziwei Liu, et al. Llava-onevision: Easy visual task transfer. *arXiv preprint arXiv:2408.03326*, 2024. 5
- [20] Dingming Li, Hongxing Li, Zixuan Wang, Yuchen Yan, Hang Zhang, Siqi Chen, Guiyang Hou, Shengpei Jiang, Wenqi Zhang, Yongliang Shen, et al. Viewspatial-bench: Evaluating multi-perspective spatial localization in vision-language models. *arXiv preprint arXiv:2505.21500*, 2025. 5
- [21] Hongxing Li, Dingming Li, Zixuan Wang, Yuchen Yan, Hang Wu, Wenqi Zhang, Yongliang Shen, Weiming Lu, Jun Xiao, and Yueting Zhuang. Spatialladder: Progressive training for spatial reasoning in vision-language models. *arXiv preprint arXiv:2510.08531*, 2025. 6
- [22] Ruilong Li, Brent Yi, Junchen Liu, Hang Gao, Yi Ma, and Angjoo Kanazawa. Cameras as relative positional encoding. *arXiv preprint arXiv:2507.10496*, 2025. 4, 8
- [23] Ji Lin, Hongxu Yin, Wei Ping, Pavlo Molchanov, Mohammad Shoeybi, and Song Han. Vila: On pre-training for visual language models. In *CVPR*, pages 26689–26699, 2024. 5
- [24] Ben Mildenhall, Pratul P Srinivasan, Matthew Tancik, Jonathan T Barron, Ravi Ramamoorthi, and Ren Ng. Nerf: Representing scenes as neural radiance fields for view synthesis. *Communications of the ACM*, 65(1):99–106, 2021. 2
- [25] Kun Ouyang, Yuanxin Liu, Haoning Wu, Yi Liu, Hao Zhou, Jie Zhou, Fandong Meng, and Xu Sun. Spacer: Reinforcing mllms in video spatial reasoning. *arXiv preprint arXiv:2504.01805*, 2025. 6
- [26] Mingjie Pan, Jiaming Liu, Renrui Zhang, Peixiang Huang, Xiaoqi Li, Hongwei Xie, Bing Wang, Li Liu, and Shanghang Zhang. Renderoc: Vision-centric 3d occupancy prediction with 2d rendering supervision. In *2024 IEEE International Conference on Robotics and Automation (ICRA)*, pages 12404–12411, 2024. 2

- [27] Julius Plücker. *Analytisch-geometrische Entwicklungen*. GD Baedeker, 1828. 8
- [28] Zhangyang Qi, Zhixiong Zhang, Ye Fang, Jiaqi Wang, and Hengshuang Zhao. Gpt4scene: Understand 3d scenes from videos with vision-language models. *arXiv preprint arXiv:2501.01428*, 2025. 2
- [29] Oriane Siméoni, Huy V Vo, Maximilian Seitzer, Federico Baldassarre, Maxime Oquab, Cijo Jose, Vasil Khalidov, Marc Szafraniec, Seungeun Yi, Michaël Ramamonjisoa, et al. Dinov3. *arXiv preprint arXiv:2508.10104*, 2025. 4, 6
- [30] Xiangyu Sun, Haoyi Jiang, Liu Liu, Seungtae Nam, Gyeongjin Kang, Xinjie Wang, Wei Sui, Zhizhong Su, Wenyu Liu, Xinggong Wang, et al. Uni3r: Unified 3d reconstruction and semantic understanding via generalizable gaussian splatting from unposed multi-view images. *arXiv preprint arXiv:2508.03643*, 2025. 2
- [31] Gemini Team, Petko Georgiev, Ving Ian Lei, Ryan Burnell, Libin Bai, Anmol Gulati, Garrett Tanzer, Damien Vincent, Zhufeng Pan, Shibo Wang, et al. Gemini 1.5: Unlocking multimodal understanding across millions of tokens of context. *arXiv preprint arXiv:2403.05530*, 2024. 5
- [32] Peter Tong, Ellis Brown, Penghao Wu, Sanghyun Woo, Adithya Jairam Vedagiri IYER, Sai Charitha Akula, Shusheng Yang, Jihan Yang, Manoj Middepogu, Ziteng Wang, et al. Cambrian-1: A fully open, vision-centric exploration of multimodal llms. *NeurIPS*, 37:87310–87356, 2024. 5
- [33] Haoru Wang, Kai Ye, Yangyan Li, Wenzheng Chen, and Baoquan Chen. The less you depend, the more you learn: Synthesizing novel views from sparse, unposed images without any 3d knowledge. *arXiv preprint arXiv:2506.09885*, 2025. 2
- [34] Jianyuan Wang, Minghao Chen, Nikita Karaev, Andrea Vedaldi, Christian Rupprecht, and David Novotny. Vgg: Visual geometry grounded transformer. In *CVPR*, pages 5294–5306, 2025. 1, 2, 4, 6
- [35] Shuzhe Wang, Vincent Leroy, Yohann Cabon, Boris Chidlovskii, and Jerome Revaud. Dust3r: Geometric 3d vision made easy. In *CVPR*, pages 20697–20709, 2024. 1, 2
- [36] Yifan Wang, Jianjun Zhou, Haoyi Zhu, Wenzheng Chang, Yang Zhou, Zizun Li, Junyi Chen, Jiangmiao Pang, Chunhua Shen, and Tong He. π^3 : Permutation-equivariant visual geometry learning. *arXiv preprint arXiv:2507.13347*, 2025. 2
- [37] Zehan Wang, Haifeng Huang, Yang Zhao, Ziang Zhang, and Zhou Zhao. Chat-3d: Data-efficiently tuning large language model for universal dialogue of 3d scenes. *arXiv preprint arXiv:2308.08769*, 2023. 2
- [38] Diankun Wu, Fangfu Liu, Yi-Hsin Hung, and Yueqi Duan. Spatial-mllm: Boosting mllm capabilities in visual-based spatial intelligence. *arXiv preprint arXiv:2505.23747*, 2025. 1, 2, 5
- [39] Jihan Yang, Shusheng Yang, Anjali W Gupta, Rilyn Han, Li Fei-Fei, and Saining Xie. Thinking in space: How multimodal large language models see, remember, and recall spaces. In *CVPR*, pages 10632–10643, 2025. 1, 2, 5
- [40] Shusheng Yang, Jihan Yang, Pinzhi Huang, Ellis Brown, Zihao Yang, Yue Yu, Shengbang Tong, Zihan Zheng, Yifan Xu, Muhan Wang, et al. Cambrian-s: Towards spatial supersensing in video. *arXiv preprint arXiv:2511.04670*, 2025. 5
- [41] Botao Ye, Sifei Liu, Haoifei Xu, Xueting Li, Marc Pollefeys, Ming-Hsuan Yang, and Songyou Peng. No pose, no problem: Surprisingly simple 3d gaussian splats from sparse unposed images. In *ICLR*, 2025. 2
- [42] Chandan Yeshwanth, Yueh-Cheng Liu, Matthias Nießner, and Angela Dai. Scannet++: A high-fidelity dataset of 3d indoor scenes. In *ICCV*, pages 12–22, 2023. 5
- [43] Alex Yu, Vickie Ye, Matthew Tancik, and Angjoo Kanazawa. pixelnerf: Neural radiance fields from one or few images. In *CVPR*, pages 4578–4587, 2021. 2
- [44] Jiahui Zhang, Yurui Chen, Yanpeng Zhou, Yueming Xu, Ze Huang, Jilin Mei, Junhui Chen, Yu-Jie Yuan, Xinyue Cai, Guowei Huang, et al. From flatland to space: Teaching vision-language models to perceive and reason in 3d. *arXiv preprint arXiv:2503.22976*, 2025. 5
- [45] Yuanhan Zhang, Jinming Wu, Wei Li, Bo Li, Zejun Ma, Ziwei Liu, and Chunyuan Li. Video instruction tuning with synthetic data. *arXiv preprint arXiv:2410.02713*, 2024. 5
- [46] Duo Zheng, Shijia Huang, Yanyang Li, and Liwei Wang. Learning from videos for 3d world: Enhancing mllms with 3d vision geometry priors. *arXiv preprint arXiv:2505.24625*, 2025. 1, 2, 5, 6